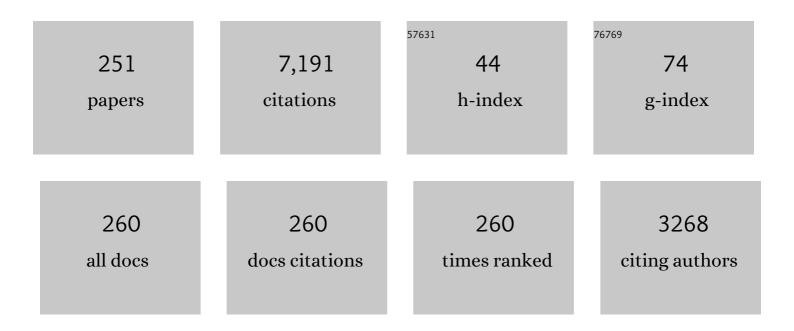
List of Publications by Year in descending order

Source: https://exaly.com/author-pdf/5927470/publications.pdf Version: 2024-02-01



CEDNOT DIANK

#	Article	IF	CITATIONS
1	Impact of anatomical reverse remodelling in the design of optimal quadripolar pacing leads: A computational study. Computers in Biology and Medicine, 2022, 140, 105073.	3.9	6
2	Parallel space-time adaptive numerical simulation of 3D cardiac electrophysiology. Applied Numerical Mathematics, 2022, 173, 295-307.	1.2	4
3	On the incorporation of obstacles in a fluid flow problem using a Navier–Stokes–Brinkman penalization approach. Journal of Computational Science, 2022, 57, 101506.	1.5	9
4	Determining anatomical and electrophysiological detail requirements for computational ventricular models of porcine myocardial infarction. Computers in Biology and Medicine, 2022, 141, 105061.	3.9	9
5	Global Sensitivity Analysis of Four Chamber Heart Hemodynamics Using Surrogate Models. IEEE Transactions on Biomedical Engineering, 2022, 69, 3216-3223.	2.5	13
6	An Integrated Workflow for Building Digital Twins of Cardiac Electromechanics—A Multi-Fidelity Approach for Personalising Active Mechanics. Mathematics, 2022, 10, 823.	1.1	16
7	Diversity and complexity of the cavotricuspid isthmus in rabbits: A novel scheme for classification and geometrical transformation of anatomical structures. PLoS ONE, 2022, 17, e0264625.	1.1	0
8	Impact of Intraventricular Septal Fiber Orientation on Cardiac Electromechanical Function. American Journal of Physiology - Heart and Circulatory Physiology, 2022, , .	1.5	5
9	Modelling the interaction between stem cells derived cardiomyocytes patches and host myocardium to aid non-arrhythmic engineered heart tissue design. PLoS Computational Biology, 2022, 18, e1010030.	1.5	8
10	An accurate, robust, and efficient finite element framework with applications to anisotropic, nearly and fully incompressible elasticity. Computer Methods in Applied Mechanics and Engineering, 2022, 394, 114887.	3.4	11
11	PO-645-01 SUBTHRESHOLD DELAYED AFTERDEPOLARIZATIONS MEDIATED BY REDUCED TISSUE COUPLING PROVIDE AN IMPORTANT SUBSTRATE FOR UNIDIRECTIONAL BLOCK AND ARRHYTHMOGENESIS IN THE INFARCT BORDER ZONE. Heart Rhythm, 2022, 19, S223-S224.	0.3	0
12	Robust and efficient fixed-point algorithm for the inverse elastostatic problem to identify myocardial passive material parameters and the unloaded reference configuration. Journal of Computational Physics, 2022, 463, 111266.	1.9	13
13	Subthreshold delayed afterdepolarizations mediated by reduced tissue conductivity form a substrate for unidirectional block and reentry within the infarcted heart. Europace, 2022, 24, .	0.7	0
14	An automated near-real time computational method for induction and treatment of scar-related ventricular tachycardias. Medical Image Analysis, 2022, 80, 102483.	7.0	5
15	Non-invasive delineation of ventricular tachycardia substrates for cardiac stereotactic body radiotherapy: utility of in-silico pace-mapping. Europace, 2022, 24, .	0.7	0
16	Automated detection of scar-related ventricular tachycardia origins from implanted device electrograms: a combined computational-AI platform. Europace, 2022, 24, .	0.7	0
17	Predicting arrhythmia recurrence following catheter ablation for ventricular tachycardia using late gadolinium enhancement magnetic resonance imaging: Implications of varying scar ranges. Heart Rhythm, 2022, 19, 1604-1610.	0.3	4
18	A coupling strategy for a first 3D-1D model of the cardiovascular system to study the effects of pulse wave propagation on cardiac function. Computational Mechanics, 2022, 70, 703-722.	2.2	4

#	Article	IF	CITATIONS
19	Late-Gadolinium Enhancement Interface Area and Electrophysiological Simulations Predict Arrhythmic Events in Patients With Nonischemic Dilated Cardiomyopathy. JACC: Clinical Electrophysiology, 2021, 7, 238-249.	1.3	13
20	PIEMAP: Personalized Inverse Eikonal Model from Cardiac Electro-Anatomical Maps. Lecture Notes in Computer Science, 2021, , 76-86.	1.0	10
21	The Effect of Ventricular Myofibre Orientation on Atrial Dynamics. Lecture Notes in Computer Science, 2021, , 659-670.	1.0	3
22	Estimation and Validation of Cardiac Conduction Velocity and Wavefront Reconstruction Using Epicardial and Volumetric Data. IEEE Transactions on Biomedical Engineering, 2021, 68, 3290-3300.	2.5	12
23	Building Models of Patient-Specific Anatomy and Scar Morphology from Clinical MRI Data. , 2021, , 453-461.		0
24	How Electrode Position Affects Selective His Bundle Capture: A Modelling Study. IEEE Transactions on Biomedical Engineering, 2021, 68, 3410-3416.	2.5	2
25	Bidomain Model of Defibrillation. , 2021, , 61-76.		3
26	Using machine learning to identify local cellular properties that support re-entrant activation in patient-specific models of atrial fibrillation. Europace, 2021, 23, i12-i20.	0.7	9
27	Learning Atrial Fiber Orientations and Conductivity Tensors from Intracardiac Maps Using Physics-Informed Neural Networks. Lecture Notes in Computer Science, 2021, 2021, 650-658.	1.0	11
28	Automatic reconstruction of the left atrium activation from sparse intracardiac contact recordings by inverse estimate of fibre structure and anisotropic conduction in a patient-specific model. Europace, 2021, 23, i63-i70.	0.7	5
29	Assessing the ability of substrate mapping techniques to guide ventricular tachycardia ablation using computational modelling. Computers in Biology and Medicine, 2021, 130, 104214.	3.9	12
30	Linking statistical shape models and simulated function in the healthy adult human heart. PLoS Computational Biology, 2021, 17, e1008851.	1.5	41
31	Quantifying the spatiotemporal influence of acute myocardial ischemia on volumetric conduction velocity. Journal of Electrocardiology, 2021, 66, 86-94.	0.4	3
32	Automated Localization of Focal Ventricular Tachycardia From Simulated Implanted Device Electrograms: A Combined Physics–Al Approach. Frontiers in Physiology, 2021, 12, 682446.	1.3	9
33	<scp>GEASI</scp> : Geodesicâ€based earliest activation sites identification in cardiac models. International Journal for Numerical Methods in Biomedical Engineering, 2021, 37, e3505.	1.0	5
34	A Framework for the generation of digital twins of cardiac electrophysiology from clinical 12-leads ECGs. Medical Image Analysis, 2021, 71, 102080.	7.0	72
35	Automated Framework for the Inclusion of a His–Purkinje System in Cardiac Digital Twins of Ventricular Electrophysiology. Annals of Biomedical Engineering, 2021, 49, 3143-3153.	1.3	24
36	B-PO03-023 HIS BUNDLE PACING ACHIEVES BETTER VENTRICULAR SYNCHRONY THAN BIVENTRICULAR PACING IN PATIENTS WITH SCAR IN THE LEFT VENTRICULAR FREE WALL. Heart Rhythm, 2021, 18, S197-S198.	0.3	1

#	Article	IF	CITATIONS
37	B-PO04-002 HIS-PURKINJE CONDUCTION SLOWING WORSENS RESPONSE TO HIS BUNDLE PACING. Heart Rhythm, 2021, 18, S280.	0.3	1
38	B-PO01-011 AUTOMATED LOCALISATION OF FOCAL VT ORIGINS USING IMPLANTED DEVICE EGMS AND CONVOLUTIONAL NEURAL NETWORKS. Heart Rhythm, 2021, 18, S55.	0.3	0
39	B-PO02-112 PATIENT SPECIFIC MODELS SHOW THE IMPORTANCE OF FIBRILLATORY-AREAS IN ATRIAL FIBRILLATION ABLATION OUTCOMES AND TREATMENT PLANNING. Heart Rhythm, 2021, 18, S142-S143.	0.3	0
40	B-PO05-005 MULTI-PHYSICS, PATIENT-SPECIFIC COMPUTATIONAL MODELING OF LA ELECTROPHYSIOLOGY, BIOMECHANICS AND HEMODYNAMICS REVEALS MECHANISTIC CONNECTIONS BETWEEN FIBROTIC REMODELING AND THROMBOSIS RISK. Heart Rhythm, 2021, 18, S372-S373.	0.3	2
41	B-IN01-01 AUTOMATED LOCALISATION OF FOCAL VT ORIGINS USING IMPLANTED DEVICE EGMS AND CONVOLUTIONAL NEURAL NETWORKS. Heart Rhythm, 2021, 18, S464.	0.3	0
42	The openCARP simulation environment for cardiac electrophysiology. Computer Methods and Programs in Biomedicine, 2021, 208, 106223.	2.6	84
43	Combining endocardial mapping and electrocardiographic imaging (ECGI) for improving PVC localization: A feasibility study. Journal of Electrocardiology, 2021, 69S, 51-54.	0.4	2
44	Non-invasive simulated electrical and measured mechanical indices predict response to cardiac resynchronization therapy. Computers in Biology and Medicine, 2021, 138, 104872.	3.9	4
45	A computationally efficient physiologically comprehensive 3D–0D closed-loop model of the heart and circulation. Computer Methods in Applied Mechanics and Engineering, 2021, 386, 114092.	3.4	26
46	Influence of Electrode Placement on the Morphology of In Silico 12 Lead Electrocardiograms. , 2021, , .		1
47	The Role of Myocardial Fiber Direction in Epicardial Activation Patterns via Uncertainty Quantification. , 2021, 48, .		4
48	Versatile stabilized finite element formulations for nearly and fully incompressible solid mechanics. Computational Mechanics, 2020, 65, 193-215.	2.2	17
49	The impact of wall thickness and curvature on wall stress in patient-specific electromechanical models of the left atrium. Biomechanics and Modeling in Mechanobiology, 2020, 19, 1015-1034.	1.4	23
50	TCT CONNECT-153 Double-Kissing Culotte Technique for Coronary Bifurcation Stenting: Technical Evaluation and Comparison With Conventional Double-Stenting Techniques. Journal of the American College of Cardiology, 2020, 76, B65.	1.2	0
51	In silico Comparison of Left Atrial Ablation Techniques That Target the Anatomical, Structural, and Electrical Substrates of Atrial Fibrillation. Frontiers in Physiology, 2020, 11, 1145.	1.3	38
52	In-silico pace-mapping using a detailed whole torso model and implanted electronic device electrograms for more efficient ablation planning. Computers in Biology and Medicine, 2020, 125, 104005.	3.9	10
53	Personalization of electro-mechanical models of the pressure-overloaded left ventricle: fitting of Windkessel-type afterload models. Philosophical Transactions Series A, Mathematical, Physical, and Engineering Sciences, 2020, 378, 20190342.	1.6	23
54	Creation and application of virtual patient cohorts of heart models. Philosophical Transactions Series A, Mathematical, Physical, and Engineering Sciences, 2020, 378, 20190558.	1.6	50

#	Article	IF	CITATIONS
55	P532Endocardial pacing is less arrhythmogenic than conventional epicardial pacing when pacing in proximity to scar in patients with ischemic heart failure. Europace, 2020, 22, .	0.7	0
56	P321Subthreshold delayed afterdepolarizations form a substrate for conduction block in the infarcted heart. Europace, 2020, 22, .	0.7	0
57	Automating image-based mesh generation and manipulation tasks in cardiac modeling workflows using Meshtool. SoftwareX, 2020, 11, 100454.	1.2	41
58	His-bundle and left bundle pacing with optimized atrioventricular delay achieve superior electrical synchrony over endocardial and epicardial pacing in left bundle branch block patients. Heart Rhythm, 2020, 17, 1922-1929.	0.3	44
59	A computational investigation into rate-dependant vectorcardiogram changes due to specific fibrosis patterns in non-isch¦mic dilated cardiomyopathy. Computers in Biology and Medicine, 2020, 123, 103895.	3.9	10
60	A publicly available virtual cohort of four-chamber heart meshes for cardiac electro-mechanics simulations. PLoS ONE, 2020, 15, e0235145.	1,1	59
61	An inverse Eikonal method for identifying ventricular activation sequences from epicardial activation maps. Journal of Computational Physics, 2020, 419, 109700.	1.9	13
62	Computational modeling of cardiac growth and remodeling in pressure overloaded hearts—Linking microstructure to organ phenotype. Acta Biomaterialia, 2020, 106, 34-53.	4.1	20
63	Simulating ventricular systolic motion in a four-chamber heart model with spatially varying robin boundary conditions to model the effect of the pericardium. Journal of Biomechanics, 2020, 101, 109645.	0.9	54
64	A coupled monodomain solver with optimal memory usage for the simulation of cardiac wave propagation. Applied Mathematics and Computation, 2020, 378, 125212.	1.4	5
65	Left ventricular endocardial pacing is less arrhythmogenic than conventional epicardial pacing when pacing in proximity to scar. Heart Rhythm, 2020, 17, 1262-1270.	0.3	16
66	3D Electrophysiological Modeling of Interstitial Fibrosis Networks and Their Role in Ventricular Arrhythmias in Non-Ischemic Cardiomyopathy. IEEE Transactions on Biomedical Engineering, 2020, 67, 3125-3133.	2.5	8
67	Direct comparison of a novel antitachycardia pacing algorithm against present methods using virtual patient modeling. Heart Rhythm, 2020, 17, 1602-1608.	0.3	26
68	Effect of Myocardial Fiber Direction on Epicardial Activation Patterns. , 2020, 47, .		1
69	Quantifying the Spatiotemporal Influence of Acute Myocardial Ischemia on Volumetric Conduction Velocity. , 2020, 47, .		1
70	Double-kissing culotte technique for coronary bifurcation stenting. EuroIntervention, 2020, 16, e724-e733.	1.4	13
71	Generation of a cohort of whole-torso cardiac models for assessing the utility of a novel computed shock vector efficiency metric for ICD optimisation. Computers in Biology and Medicine, 2019, 112, 103368.	3.9	13
72	A rule-based method for predicting the electrical activation of the heart with cardiac resynchronization therapy from non-invasive clinical data. Medical Image Analysis, 2019, 57, 197-213.	7.0	36

#	Article	IF	CITATIONS
73	Inverse localization of earliest cardiac activation sites from activation maps based on the viscous Eikonal equation. Journal of Mathematical Biology, 2019, 79, 2033-2068.	0.8	6
74	Factors Promoting Conduction Slowing as Substrates for Block and Reentry in Infarcted Hearts. Biophysical Journal, 2019, 117, 2361-2374.	0.2	31
75	Scar shape analysis and simulated electrical instabilities in a non-ischemic dilated cardiomyopathy patient cohort. PLoS Computational Biology, 2019, 15, e1007421.	1.5	10
76	Sex-Dependent QRS Guidelines for Cardiac Resynchronization Therapy Using Computer Model Predictions. Biophysical Journal, 2019, 117, 2375-2381.	0.2	14
77	Cardiac Modeling. , 2019, , 1-20.		1
78	Pacing in proximity to scar during cardiac resynchronization therapy increases local dispersion of repolarization and susceptibility to ventricular arrhythmogenesis. Heart Rhythm, 2019, 16, 1475-1483.	0.3	42
79	The Left and Right Ventricles Respond Differently to Variation of Pacing Delays in Cardiac Resynchronization Therapy: A Combined Experimental- Computational Approach. Frontiers in Physiology, 2019, 10, 17.	1.3	21
80	Parallel and space-time adaptivity for the numerical simulation of cardiac action potentials. Applied Mathematics and Computation, 2019, 353, 406-417.	1.4	6
81	Validation study of computational fluid dynamics models of hemodynamics in the human aorta. Proceedings in Applied Mathematics and Mechanics, 2019, 19, e201900472.	0.2	3
82	Validation of Intramural Wavefront Reconstruction and Estimation of 3D Conduction Velocity. , 2019, 46, .		1
83	Personalized computational modeling of left atrial geometry and transmural myofiber architecture. Medical Image Analysis, 2018, 47, 180-190.	7.0	46
84	Universal ventricular coordinates: A generic framework for describing position within the heart and transferring data. Medical Image Analysis, 2018, 45, 83-93.	7.0	66
85	A work flow to build and validate patient specific left atrium electrophysiology models from catheter measurements. Medical Image Analysis, 2018, 47, 153-163.	7.0	36
86	Fibrosis Microstructure Modulates Reentry in Non-ischemic Dilated Cardiomyopathy: Insights From Imaged Guided 2D Computational Modeling. Frontiers in Physiology, 2018, 9, 1832.	1.3	25
87	Assessment of wall stresses and mechanical heart power in the left ventricle: Finite element modeling versus Laplace analysis. International Journal for Numerical Methods in Biomedical Engineering, 2018, 34, e3147.	1.0	23
88	Arterial hypertension drives arrhythmia progression via specific structural remodeling in a porcine model of atrial fibrillation. Heart Rhythm, 2018, 15, 1328-1336.	0.3	19
89	Microscopic Isthmuses and Fibrosis Within the Border Zone of Infarcted Hearts Promote Calcium-Mediated Ectopy and Conduction Block. Frontiers in Physics, 2018, 6, .	1.0	26
90	Modeling the Electrophysiological Properties of the Infarct Border Zone. Frontiers in Physiology, 2018, 9, 356.	1.3	72

#	Article	IF	CITATIONS
91	Towards a Computational Framework for Modeling the Impact of Aortic Coarctations Upon Left Ventricular Load. Frontiers in Physiology, 2018, 9, 538.	1.3	24
92	Numerical analysis for an optimal control of bidomain-bath model. Journal of Differential Equations, 2017, 263, 2419-2456.	1.1	3
93	Efficient computation of electrograms and ECGs in human whole heart simulations using a reaction-eikonal model. Journal of Computational Physics, 2017, 346, 191-211.	1.9	109
94	Biophysical Modeling to Determine the Optimization of Left Ventricular Pacing Site and AV/VV Delays in the Acute and Chronic Phase of Cardiac Resynchronization Therapy. Journal of Cardiovascular Electrophysiology, 2017, 28, 208-215.	0.8	25
95	Stochastic spontaneous calcium release events and sodium channelopathies promote ventricular arrhythmias. Chaos, 2017, 27, 093910.	1.0	19
96	Highly trabeculated structure of the human endocardium underlies asymmetrical response to low-energy monophasic shocks. Chaos, 2017, 27, 093913.	1.0	6
97	Primal-dual active set strategy for large scale optimization of cardiac defibrillation. Applied Mathematics and Computation, 2017, 292, 178-193.	1.4	8
98	P1707Interatrial differences in AF remodelling. Europace, 2017, 19, iii367-iii368.	0.7	0
99	<i>In-vitro</i> experiments to characterize ventricular electromechanics. Current Directions in Biomedical Engineering, 2016, 2, 263-266.	0.2	0
100	PDE constrained optimization of electrical defibrillation in a 3D ventricular slice geometry. International Journal for Numerical Methods in Biomedical Engineering, 2016, 32, e02742.	1.0	5
101	Patient-specific modeling of left ventricular electromechanics as a driver for haemodynamic analysis. Europace, 2016, 18, iv121-iv129.	0.7	32
102	Analysis of lead placement optimization metrics in cardiac resynchronization therapy with computational modelling. Europace, 2016, 18, iv113-iv120.	0.7	7
103	The relative role of patient physiology and device optimisation in cardiac resynchronisation therapy: A computational modelling study. Journal of Molecular and Cellular Cardiology, 2016, 96, 93-100.	0.9	38
104	Balloon Dilatation and Stenting for Aortic Coarctation. Circulation: Cardiovascular Interventions, 2016, 9, .	1.4	40
105	A 3D boundary optimal control for the bidomain-bath system modeling the thoracic shock therapy for cardiac defibrillation. Journal of Mathematical Analysis and Applications, 2016, 437, 972-998.	0.5	10
106	Image-Based Personalization of Cardiac Anatomy for Coupled Electromechanical Modeling. Annals of Biomedical Engineering, 2016, 44, 58-70.	1.3	48
107	Anatomically accurate high resolution modeling of human whole heart electromechanics: A strongly scalable algebraic multigrid solver method for nonlinear deformation. Journal of Computational Physics, 2016, 305, 622-646.	1.9	115
108	Three-dimensional atrial wall thickness maps to inform catheter ablation procedures for atrial fibrillation. Europace, 2016, 18, 376-383.	0.7	59

#	Article	IF	CITATIONS
109	Investigating a Novel Activation-Repolarisation Time Metric to Predict Localised Vulnerability to Reentry Using Computational Modelling. PLoS ONE, 2016, 11, e0149342.	1.1	30
110	Verification of cardiac mechanics software: benchmark problems and solutions for testing active and passive material behaviour. Proceedings of the Royal Society A: Mathematical, Physical and Engineering Sciences, 2015, 471, 20150641.	1.0	80
111	A multiscale computational model of spatially resolved calcium cycling in cardiac myocytes: from detailed cleft dynamics to the whole cell concentration profiles. Frontiers in Physiology, 2015, 6, 255.	1.3	15
112	Beneficial Effect on Cardiac Resynchronization From Left Ventricular Endocardial Pacing Is Mediated by Early Access to High Conduction Velocity Tissue. Circulation: Arrhythmia and Electrophysiology, 2015, 8, 1164-1172.	2.1	47
113	Stochastic spontaneous calcium release events trigger premature ventricular complexes by overcoming electrotonic load. Cardiovascular Research, 2015, 107, 175-183.	1.8	41
114	Application of optimal control to the cardiac defibrillation problem using a physiological model of cellular dynamics. Applied Numerical Mathematics, 2015, 95, 130-139.	1.2	1
115	Biophotonic Modelling of Cardiac Optical Imaging. Advances in Experimental Medicine and Biology, 2015, 859, 367-404.	0.8	1
116	Local Gradients in Electrotonic Loading Modulate the Local Effective Refractory Period: Implications for Arrhythmogenesis in the Infarct Border Zone. IEEE Transactions on Biomedical Engineering, 2015, 62, 2251-2259.	2.5	23
117	Bidomain Model: Applications. , 2015, , 119-125.		0
118	Structural Heterogeneity Modulates Effective Refractory Period: A Mechanism of Focal Arrhythmia Initiation. PLoS ONE, 2014, 9, e109754.	1.1	22
119	Simulating photon scattering effects in structurally detailed ventricular models using a Monte Carlo approach. Frontiers in Physiology, 2014, 5, 338.	1.3	16
120	Sensitivity and Specificity of Substrate Mapping: An <i>In Silico</i> Framework for the Evaluation of Electroanatomical Substrate Mapping Strategies. Journal of Cardiovascular Electrophysiology, 2014, 25, 774-780.	0.8	14
121	Influence of the Purkinje-muscle junction on transmural repolarization heterogeneity. Cardiovascular Research, 2014, 103, 629-640.	1.8	30
122	Effects of Regional Mitochondrial Depolarization on Electrical Propagation. Circulation: Arrhythmia and Electrophysiology, 2014, 7, 143-151.	2.1	60
123	An Efficient Finite Element Approach for Modeling Fibrotic Clefts in the Heart. IEEE Transactions on Biomedical Engineering, 2014, 61, 900-910.	2.5	56
124	Mechanism of reentry induction by a 9-V battery in rabbit ventricles. American Journal of Physiology - Heart and Circulatory Physiology, 2014, 306, H1041-H1053.	1.5	7
125	Boundary control of bidomain equations with state-dependent switching source functions in the ionic model. Journal of Computational Physics, 2014, 273, 227-242.	1.9	2
126	Stepping into Fully GPU Accelerated Biomedical Applications. Lecture Notes in Computer Science, 2014, , 3-14.	1.0	2

#	Article	IF	CITATIONS
127	Optimal control approach to termination of re-entry waves in cardiac electrophysiology. Journal of Mathematical Biology, 2013, 67, 359-388.	0.8	22
128	Influence of myocardial fiber/sheet orientations on left ventricular mechanical contraction. Mathematics and Mechanics of Solids, 2013, 18, 592-606.	1.5	93
129	Electroanatomical Characterization of Atrial Microfibrosis in a Histologically Detailed Computer Model. IEEE Transactions on Biomedical Engineering, 2013, 60, 2339-2349.	2.5	32
130	On boundary stimulation and optimal boundary control of the bidomain equations. Mathematical Biosciences, 2013, 245, 206-215.	0.9	9
131	Mechanistic Inquiry into the Role of Tissue Remodeling in Fibrotic Lesions in Human Atrial Fibrillation. Biophysical Journal, 2013, 104, 2764-2773.	0.2	113
132	Elastic Registration of Edges Using Diffuse Surfaces. Lecture Notes in Computational Vision and Biomechanics, 2013, , 261-282.	0.5	1
133	Tissue Structure and Ca2+-Mediated Ectopic Beats. Biomedizinische Technik, 2013, 58 Suppl 1, .	0.9	0
134	The functional role of electrophysiological heterogeneity in the rabbit ventricle during rapid pacing and arrhythmias. American Journal of Physiology - Heart and Circulatory Physiology, 2013, 304, H1240-H1252.	1.5	24
135	Modeling the dispersion in electromechanically coupled myocardium. International Journal for Numerical Methods in Biomedical Engineering, 2013, 29, 1267-1284.	1.0	64
136	Parametrization strategies for matching activation sequences in models of ventricular electrophysiology - Withdrawn. , 2013, 2013, 1534-7.		0
137	Computational Challenges in Building Multi-Scale and Multi-Physics Models of Cardiac Electro-Mechanics. Biomedizinische Technik, 2013, 58 Suppl 1, .	0.9	1
138	Simulating the Mechanics of Myocardial Tissue Using Strongly Scalable Parallel Algorithms. Biomedizinische Technik, 2013, 58 Suppl 1, .	0.9	0
139	Tachycardia in Post-Infarction Hearts: Insights from 3D Image-Based Ventricular Models. PLoS ONE, 2013, 8, e68872.	1.1	84
140	Automatic Parameterization Strategy for Cardiac Electrophysiology Simulations. Computing in Cardiology, 2013, 40, 373-376.	0.4	22
141	Investigating the Role of the Coronary Vasculature in the Mechanisms of Defibrillation. Circulation: Arrhythmia and Electrophysiology, 2012, 5, 210-219.	2.1	25
142	Decomposition of fractionated local electrograms using an analytic signal model based on sigmoid functions. Biomedizinische Technik, 2012, 57, 371-82.	0.9	4
143	Integration of different cardiac electrophysiological models into a single simulation pipeline. , 2012, ,		0
144	Subject specific, image based analysis and modeling in patients with atrial fibrillation from MRI. , 2012, ,		0

#	Article	IF	CITATIONS
145	Spongious Hypertrophic Cardiomyopathy in Patients With Mutations in the Four-and-a-Half LIM Domain 1 Gene. Circulation: Cardiovascular Genetics, 2012, 5, 490-502.	5.1	20
146	A Novel Rule-Based Algorithm for Assigning Myocardial Fiber Orientation to Computational Heart Models. Annals of Biomedical Engineering, 2012, 40, 2243-2254.	1.3	399
147	Threeâ€dimensional mechanisms of increased vulnerability to electric shocks in myocardial infarction: Altered virtual electrode polarizations and conduction delay in the periâ€infarct zone. Journal of Physiology, 2012, 590, 4537-4551.	1.3	42
148	Methodology for patient-specific modeling of atrial fibrosis as a substrate for atrial fibrillation. Journal of Electrocardiology, 2012, 45, 640-645.	0.4	112
149	Influence of ischemic core muscle fibers on surface depolarization potentials in superfused cardiac tissue preparations: a simulation study. Medical and Biological Engineering and Computing, 2012, 50, 461-472.	1.6	20
150	Biophysical Modeling to Simulate the Response to Multisite Left Ventricular Stimulation Using a Quadripolar Pacing Lead. PACE - Pacing and Clinical Electrophysiology, 2012, 35, 204-214.	0.5	72
151	Accelerating Cardiac Bidomain Simulations Using Graphics Processing Units. IEEE Transactions on Biomedical Engineering, 2012, 59, 2281-2290.	2.5	57
152	The role of fineâ€scale anatomical structure in the dynamics of reentry in computational models of the rabbit ventricles. Journal of Physiology, 2012, 590, 4515-4535.	1.3	71
153	Analyses of the Redistribution of Work following Cardiac Resynchronisation Therapy in a Patient Specific Model. PLoS ONE, 2012, 7, e43504.	1.1	20
154	The Dependence of Clinical Metrics of Cardiac Function on Lead Position in Cardiac Resynchronization Therapy: A Biophysical Modeling Study. , 2012, , 9-17.		0
155	A finite element approach for modeling micro-structural discontinuities in the heart. , 2011, 2011, 437-40.		4
156	Regional Mitochondrial Depolarization Causes Spontaneous Ventricular Arrhythmia in Cardiac Tissue. Biophysical Journal, 2011, 100, 435a-436a.	0.2	0
157	The Role of Photon Scattering in Voltage-Calcium Fluorescent Recordings of Ventricular Fibrillation. Biophysical Journal, 2011, 101, 307-318.	0.2	9
158	Cardiac Bidomain Bath-Loading Effects during Arrhythmias: Interaction with Anatomical Heterogeneity. Biophysical Journal, 2011, 101, 2871-2881.	0.2	31
159	Modeling Defibrillation of the Heart: Approaches and Insights. IEEE Reviews in Biomedical Engineering, 2011, 4, 89-102.	13.1	36
160	Simulating Human Cardiac Electrophysiology on Clinical Time-Scales. Frontiers in Physiology, 2011, 2, 14.	1.3	105
161	Inter-model consistency and complementarity: Learning from ex-vivo imaging and electrophysiological data towards an integrated understanding of cardiac physiology. Progress in Biophysics and Molecular Biology, 2011, 107, 122-133.	1.4	35
162	A Macro Finite-Element Formulation for Cardiac Electrophysiology Simulations Using Hybrid Unstructured Grids. IEEE Transactions on Biomedical Engineering, 2011, 58, 1055-1065.	2.5	41

#	Article	IF	CITATIONS
163	Representing Cardiac Bidomain Bath-Loading Effects by an Augmented Monodomain Approach: Application to Complex Ventricular Models. IEEE Transactions on Biomedical Engineering, 2011, 58, 1066-1075.	2.5	59
164	Estimation of Local Orientations in Fibrous Structures With Applications to the Purkinje System. IEEE Transactions on Biomedical Engineering, 2011, 58, 1762-1772.	2.5	6
165	Bidomain ECG Simulations Using an Augmented Monodomain Model for the Cardiac Source. IEEE Transactions on Biomedical Engineering, 2011, 58, 2297-2307.	2.5	56
166	Numerical solution for optimal control ofÂtheÂreaction-diffusion equations in cardiac electrophysiology. Computational Optimization and Applications, 2011, 49, 149-178.	0.9	44
167	A Coupled Model for the Left Ventricle Including Regional Differences in Structure. Proceedings in Applied Mathematics and Mechanics, 2011, 11, 85-86.	0.2	1
168	Accelerating cardiac excitation spread simulations using graphics processing units. Concurrency Computation Practice and Experience, 2011, 23, 708-720.	1.4	31
169	Verification of cardiac tissue electrophysiology simulators using an <i>N</i> -version benchmark. Philosophical Transactions Series A, Mathematical, Physical, and Engineering Sciences, 2011, 369, 4331-4351.	1.6	253
170	Length-dependent tension in the failing heart and the efficacy of cardiac resynchronization therapy. Cardiovascular Research, 2011, 89, 336-343.	1.8	133
171	Modeling Atrial Fiber Orientation in Patient-Specific Geometries: A Semi-automatic Rule-Based Approach. Lecture Notes in Computer Science, 2011, , 223-232.	1.0	59
172	Purkinje-mediated Effects in the Response of Quiescent Ventricles to Defibrillation Shocks. Annals of Biomedical Engineering, 2010, 38, 456-468.	1.3	39
173	Imageâ€based models of cardiac structure in health and disease. Wiley Interdisciplinary Reviews: Systems Biology and Medicine, 2010, 2, 489-506.	6.6	113
174	Development of an anatomically detailed MRI-derived rabbit ventricular model and assessment of its impact on simulations of electrophysiological function. American Journal of Physiology - Heart and Circulatory Physiology, 2010, 298, H699-H718.	1.5	192
175	A 2D-computer model of atrial tissue based on histographs describes the electro-anatomical impact of microstructure on endocardiac potentials and electric near-fields. , 2010, 2010, 2541-4.		7
176	Modeling Cardiac Electrophysiology at the Organ Level in the Peta FLOPS Computing Age. AIP Conference Proceedings, 2010, , .	0.3	3
177	Modeling the Role of the Coronary Vasculature During External Field Stimulation. IEEE Transactions on Biomedical Engineering, 2010, 57, 2335-2345.	2.5	49
178	A Parallel Algebraic Multigrid Solver on Graphics Processing Units. Lecture Notes in Computer Science, 2010, , 38-47.	1.0	39
179	Numerical Solutions for Optimal Control of Monodomain Equations in Cardiac Electrophysiology. , 2010, , 409-418.		2
180	Simulations of the Electrical Activity in the Heart with Graphic Processing Units. Lecture Notes in Computer Science, 2010, , 439-448.	1.0	4

#	Article	IF	CITATIONS
181	Generic Conduction Parameters for Predicting Activation Waves in Customised Cardiac Electrophysiology Models. Lecture Notes in Computer Science, 2010, , 252-260.	1.0	7
182	Near-real-time simulations of biolelectric activity in small mammalian hearts using graphical processing units. , 2009, 2009, 3290-3.		19
183	Estimation of multimodal orientation distribution functions from cardiac MRI for tracking Purkinje fibers through branchings. , 2009, , .		3
184	Image-based models of cardiac structure with applications in arrhythmia and defibrillation studies. Journal of Electrocardiology, 2009, 42, 157.e1-157.e10.	0.4	75
185	Automatically Generated, Anatomically Accurate Meshes for Cardiac Electrophysiology Problems. IEEE Transactions on Biomedical Engineering, 2009, 56, 1318-1330.	2.5	124
186	Solving the Coupled System Improves Computational Efficiency of the Bidomain Equations. IEEE Transactions on Biomedical Engineering, 2009, 56, 2404-2412.	2.5	23
187	Numerical solutions for optimal control of monodomain equations. Proceedings in Applied Mathematics and Mechanics, 2009, 9, 609-610.	0.2	1
188	Towards predictive modelling of the electrophysiology of the heart. Experimental Physiology, 2009, 94, 563-577.	0.9	110
189	Low Energy Defibrillation in Human Cardiac Tissue: A Simulation Study. Biophysical Journal, 2009, 96, 1364-1373.	0.2	33
190	Bidomain Model of Defibrillation. , 2009, , 85-109.		3
191	Effects Of Mitochondrial Depolarization On Cardiac Electrical Activity In An Integrated Multiscale Model Of The Myocardium. Biophysical Journal, 2009, 96, 663a-664a.	0.2	1
192	Arrhythmogenic mechanisms of the Purkinje system during electric shocks: A modeling study. Heart Rhythm, 2009, 6, 1782-1789.	0.3	41
193	Generation of histo-anatomically representative models of the individual heart: tools and application. Philosophical Transactions Series A, Mathematical, Physical, and Engineering Sciences, 2009, 367, 2257-2292.	1.6	135
194	The Role of Blood Vessels in Rabbit Propagation Dynamics and Cardiac Arrhythmias. Lecture Notes in Computer Science, 2009, , 268-276.	1.0	11
195	The Contribution of Core Muscle Fibers to the Surface Depolarization Signals on Cable-Like Cardiac Tissue Preparations - A Computer Simulation Study. IFMBE Proceedings, 2009, , 2077-2080.	0.2	Ο
196	Heterogeneity of Micro- and Macro-conduction in Atrial Pectinate Muscles studied with Cardiac Near Field Measurements and Computer Simulation. IFMBE Proceedings, 2009, , 559-562.	0.2	1
197	Solvers for the cardiac bidomain equations. Progress in Biophysics and Molecular Biology, 2008, 96, 3-18.	1.4	292
198	Evaluating Intramural Virtual Electrodes in the Myocardial Wedge Preparation: Simulations of Experimental Conditions. Biophysical Journal, 2008, 94, 1904-1915.	0.2	40

#	Article	IF	CITATIONS
199	Role of Purkinje system in cardiac arrhythmias. , 2008, 2008, 149-52.		1
200	Modeling the influence of the VV delay for CRT on the electrical activation patterns in absence of conduction through the AV node. , 2008, , .		0
201	Assessing influence of conductivity in heart modelling with the aim of studying cardiovascular diseases. Proceedings of SPIE, 2008, , .	0.8	7
202	Feedback control of resonant drift as a tool for low voltage defibrillation. , 2008, , .		0
203	Nonlinear filtering for extracting orientation and tracing tubular structures in 2-D medical images. , 2008, , .		2
204	From mitochondrial ion channels to arrhythmias in the heart: computational techniques to bridge the spatio-temporal scales. Philosophical Transactions Series A, Mathematical, Physical, and Engineering Sciences, 2008, 366, 3381-3409.	1.6	126
205	A Finite Element Formulation for Atrial Tissue Monolayer. Methods of Information in Medicine, 2008, 47, 131-139.	0.7	6
206	High Performance Computer Simulations of Cardiac Electrical Function Based on High Resolution MRI Datasets. Lecture Notes in Computer Science, 2008, , 571-580.	1.0	8
207	AN ITERATIVE METHOD FOR REGISTRATION OF HIGH-RESOLUTION CARDIAC HISTOANATOMICAL AND MRI IMAGES. , 2007, , .		5
208	Oblique Propagation of Activation Allows the Detection of Uncoupling Microstructures from Cardiac Near Field Behavior. Annual International Conference of the IEEE Engineering in Medicine and Biology Society, 2007, 2007, 415-8.	0.5	2
209	A Hilbert-order multiplication scheme for unstructured sparse matrices. International Journal of Parallel, Emergent and Distributed Systems, 2007, 22, 213-220.	0.7	28
210	Arrhythmogenesis Research: A Perspective from Computational Electrophysiology Viewpoint. Annual International Conference of the IEEE Engineering in Medicine and Biology Society, 2007, 2007, 406-9.	0.5	0
211	Accuracy of Local Conduction Velocity Determination from Non-Fractionated Cardiac Activation Signals. Annual International Conference of the IEEE Engineering in Medicine and Biology Society, 2007, 2007, 27-30.	0.5	5
212	Algebraic Multigrid Preconditioner for the Cardiac Bidomain Model. IEEE Transactions on Biomedical Engineering, 2007, 54, 585-596.	2.5	138
213	Reduced-Order Preconditioning for Bidomain Simulations. IEEE Transactions on Biomedical Engineering, 2007, 54, 938-942.	2.5	3
214	P1-14. Heart Rhythm, 2006, 3, S112.	0.3	0
215	P1-13. Heart Rhythm, 2006, 3, S111-S112.	0.3	4
216	P5-22. Heart Rhythm, 2006, 3, S267.	0.3	0

#	Article	IF	CITATIONS
217	What have we learned from mathematical models of defibrillation and postshock arrhythmogenesis? Application of bidomain simulations. Heart Rhythm, 2006, 3, 1232-1235.	0.3	32
218	A new floating sensor array to detect electric near fields of beating heart preparations. Biosensors and Bioelectronics, 2006, 21, 2232-2239.	5.3	27
219	Three-Dimensional Models of Individual Cardiac Histoanatomy: Tools and Challenges. Annals of the New York Academy of Sciences, 2006, 1080, 301-319.	1.8	89
220	Accelerating Large Cardiac Bidomain Simulations by Arnoldi Preconditioning. , 2006, 2006, 3923-6.		1
221	USING MONODOMAIN COMPUTER MODELS FOR THE SIMULATION OF ELECTRIC FIELDS DURING EXCITATION SPREAD IN CARDIAC TISSUE. , 2006, , 225-278.		0
222	Accelerating Large Cardiac Bidomain Simulations by Arnoldi Preconditioning. Annual International Conference of the IEEE Engineering in Medicine and Biology Society, 2006, , .	0.5	0
223	Defibrillation Depends on Conductivity Fluctuations and the Degree of Disorganization in Reentry Patterns. Journal of Cardiovascular Electrophysiology, 2005, 16, 205-216.	0.8	51
224	Preconditioning Techniques for the Bidomain Equations. Lecture Notes in Computational Science and Engineering, 2005, , 571-580.	0.1	16
225	Parallel Multigrid Preconditioner for the Cardiac Bidomain Model. IEEE Transactions on Biomedical Engineering, 2004, 51, 1960-1968.	2.5	125
226	The Shock Energy Required for Successful Defibrillation Depends on the Degree of Disorganization of the Reentrant Activation Pattern. Cardiovascular Engineering (Dordrecht, Netherlands), 2004, 4, 149-153.	1.0	1
227	GOCE Gravity Field Processing Strategy. Studia Geophysica Et Geodaetica, 2004, 48, 289-309.	0.3	10
228	Use of Cardiac Electric Near-Field Measurements to Determine Activation Times. Annals of Biomedical Engineering, 2003, 31, 1066-1076.	1.3	9
229	Cardiac Near-Field Morphology During Conduction Around a Microscopic Obstacle—A Computer Simulation Study. Annals of Biomedical Engineering, 2003, 31, 1206-1212.	1.3	6
230	Computational tools for modeling electrical activity in cardiac tissue. Journal of Electrocardiology, 2003, 36, 69-74.	0.4	292
231	Assessment of three numerical solution strategies for gravity field recovery from GOCE satellite gravity gradiometry implemented on a parallel platform. Journal of Geodesy, 2002, 76, 462-474.	1.6	65
232	Spatially restricted data distributions on the sphere: the method of orthonormalized functions and applications. Journal of Geodesy, 2001, 75, 44-56.	1.6	29
233	Model Study of Vector-Loop Morphology During Electrical Mapping of Microscopic Conduction in Cardiac Tissue. Annals of Biomedical Engineering, 2000, 28, 1244-1252.	1.3	19
234	Comparison between the role of discontinuities in cardiac conduction and in a one-dimensional hardware model. Physical Review E, 1999, 59, 5962-5969.	0.8	11

#	ARTICLE	IF	CITATIONS
235	A new real-time mapping system to detect microscopic cardiac excitation patterns. Biomedical Instrumentation and Technology, 1999, 33, 455-61.	0.2	2
236	Electro-anatomical characterization by cardiac electric near-fields. , 0, , .		0
237	Computer simulation of electric fields at the junction terminal crest -pectinate muscle. , 0, , .		0
238	Normal and fractionated cardiac near fields and their relation to microstructure - an experimental approach. , 0, , .		3
239	Modeling Defibrillation. , 0, , .		0
240	Model-based Estimation of Internal Heart Power in Aortic Valve Disease Patients , 0, , .		0
241	Patient-specific Parameterization of Left-ventricular Model of Cardiac Electrophysiology using Electrocardiographic Recordings. , 0, , .		1
242	Automatic Generation of Bi-Ventricular Models of Cardiac Electrophysiology for Patient Specific Personalization Using Non-Invasive Recordings. , 0, , .		14
243	openCARP: An Open Sustainable Framework for In-Silico Cardiac Electrophysiology Research. , 0, , .		8
244	Constructing Virtual Patient Cohorts for Simulating Atrial Fibrillation Ablation. , 0, , .		1
245	Comparison of numerical solution strategies for gravity field recovery from GOCE SGG observations implemented on a parallel platform. Advances in Geosciences, 0, 1, 39-45.	12.0	2
246	Personalized Modeling Pipeline for Left Atrial Electromechanics. , 0, , .		0
247	A Multiscale Computational Model of Calcium-Mediated Ectopy in the Human Postinfarction Heart. , 0, , .		0
248	The Effects of Non-ischemic Fibrosis Texture and Density on Mechanisms of Reentry. , 0, , .		0
249	Personalized Modelling Pipeline for Cardiac Electrophysiology Simulations of Cardiac Resynchronization Therapy in Infarct patients. , 0, , .		0
250	Predicting Activation Patterns in Cardiac Resynchronization Therapy Patients. , 0, , .		0
251	His Bundle Pacing but not Left Bundle Pacing Corrects Septal Flash in Left Bundle Branch Block Patients. , 0, , .		2